

Lattice Parameters and Local Lattice Distortions in fcc-Ni Solutions

TAO WANG, LONG-QING CHEN, and ZI-KUI LIU

The lattice parameters and the local lattice distortions around solute atoms in fcc-Ni solutions were studied using first-principles calculations. The solute atoms considered include Al, Co, Cr, Hf, Mo, Nb, Re, Ru, Ta, Ti, and W. The calculations were performed using supercells with 1 solute atom and 107 solvent atoms. It is found that the atomic size difference, the electronic interactions, and the magnetic spin relations between the solute and solvent atoms all contribute to the lattice distortions. Based on the results from first-principles calculations, the linear composition coefficients of fcc Ni lattice parameter for different solutes were determined, and the lattice parameters of multicomponent Ni-base superalloys as a function of solute composition were predicted. The results are compared with existing experimental measurements, and good agreements are obtained for both the compositional dependence of lattice parameters and the local lattice distortions.

DOI: 10.1007/s11661-007-9091-z

© The Minerals, Metals & Materials Society and ASM International 2007

I. INTRODUCTION

THE magnitude and sign of the lattice mismatch between the γ (fcc) and the γ' ($L1_2$) phases are important parameters affecting the microstructure evolution and creep strength of Ni-base superalloys. For example, the sign of the lattice mismatch dictates the orientation of the γ' precipitates under an external stress field, and the magnitude of lattice mismatch has a strong effect on the morphology of the γ' particles. Lattice parameter data are typically obtained experimentally by diffraction measurements (X-ray, neutron, etc.). They are usually scattered because of their sensitivity to the details of alloy processing.^[1] Those uncertainties may sometimes even lead to a change in the sign of the lattice mismatch.

Recently, we^[1] proposed a phenomenological model to describe the lattice parameter of an alloy as a function of temperature and composition. In particular, it was applied to Ni-Al binary alloys, and a self-consistent lattice parameter database was constructed. The model parameters were evaluated using a large amount of experimental data. However, in general, the availability of experimental data on lattice parameters of alloys is very limited. Very often there are poor agreements among experimental data from different sources. As a result, extracting modeling parameters based on experimental data alone can be difficult.

In the last decade, the quality of first-principles calculations of electronic and structural properties has improved considerably. For most cases, the reliable

formation energy of alloys and compounds and band structures can be calculated at 0 K. In this article, we use the first-principles approach to fundamentally understand local and macroscopic lattice distortions caused by various solute additions in the γ phase of Ni-base superalloys, and the purpose of this work is to establish a computational approach for predicting the effect of alloying elements on lattice parameters. Ten commonly used alloying elements in Ni-base alloys were chosen, namely, Al, Co, Cr, Hf, Mo, Nb, Re, Ru, Ta, Ti, and W. The goal is to predict the lattice parameter changes in fcc-Ni binary and multicomponent alloys as a function of temperature and composition. The results will be compared with available experimental measurements.

II. FIRST-PRINCIPLES CALCULATIONS

The first-principles calculations of the lattice parameter were performed using the Vienna *ab initio* simulation package VASP (version 4.6),^[2] which allows one to minimize the total energy with respect to the volume and shape of the cell and the positions of atoms within the cell. In the present calculations, ultrasoft pseudopotentials and the generalized gradient approximation (GGA)^[3] are adopted. The GGA partially corrects the overbinding problem of the local density approximation (LDA),^[4] and thus improves the predictions for the equilibrium volumes.^[5,6] Supercells were employed to study the lattice distortions caused by solute atoms. A test by Sandberg *et al.*^[7] indicated that a supercell of 80 atoms was needed to achieve a convergence for the formation energy of a single defect to be within 0.01 eV. We employ 108-atom supercells, a $3 \times 3 \times 3$ cubic representation of the fcc structure, with one solute atom in each supercell. The magnetism was taken into account for Ni, Co, and Cr during the calculations. To simulate

TAO WANG, Post Doctorate, LONG-QING CHEN, Professor, and ZI-KUI LIU, Professor, are with the Department of Materials Science and Engineering, The Pennsylvania State University, University Park, PA 16802, USA. TAO WANG, Post Doctorate, is with the Department of Materials Science and Engineering, Iowa State University, Ames, IA 50011, USA. Contact e-mail: taowang@iastate.edu
Manuscript submitted June 27, 2006.
Article published online April 11, 2007.

the antiferromagnetic property of Cr, at least two Cr atoms are required in the supercell, and thus a much larger supercell and several configurations need to be considered. Instead of performing such demanding calculations, two calculations were performed, both with 107 Ni atoms and 1 Cr atom. In the first case, the Cr possesses the same spin direction as the surrounding Ni atoms, which is named as "Cr₊". In the second case, the spin direction of the Cr atom is opposite to that of Ni atoms, which is denoted by "Cr₋". The set of *k* points is adapted to the size of the primitive cell, and a 4×4×4 *k*-point mesh is selected for the supercell used in the present calculations. The energy cutoff is determined by the choice of "high accuracy" in the VASP, *i.e.*, 314.1 eV for alloys in this work, which guarantees that the absolute energies are converged to a few meV.^[8] For a detailed description of the technical features and the computational procedure of the VASP calculations, we refer to the VASP manual.^[8]

Table I. Total Energies and Lattice Parameters for Ni₁₀₇X₁ fcc Solutions from First-Principles Calculations; the Lattice Parameters are One Third of the Size Dimensions of Those Supercells

X	Total Energy (eV)	Lattice Parameter (Å)	
		<i>a</i>	Δ <i>a</i>
Ni	-592.090	3.5321	—
Al	-591.859	3.5335	0.00147
Co	-593.699	3.5322	0.00012
Cr ₊	-595.920	3.5338	0.00168
Cr ₋	-595.694	3.5320	-0.00008
Hf	-597.830	3.5398	0.00775
Mo	-597.299	3.5358	0.00375
Nb	-597.401	3.5377	0.00567
Re	-598.553	3.5357	0.00361
Ru	-595.273	3.5357	0.00362
Ta	-599.390	3.5375	0.00543
Ti	-595.827	3.5352	0.00314
W	-599.508	3.5359	0.00379

Table II. Atomic Radii and Linear Regression Coefficients of Solute Atoms in fcc Ni

Solute Atom	Atomic Radius, (Å) ^[9]	Linear Regression Coefficients (Å/At. Pct)				
		45	46	23	47	Present Work
Ni	1.24	—	—	—	—	—
Al	1.43	0.183	0.185	0.194	0.100	0.1587
Co	1.25	0.024	0.020	0.020	0.081	0.0132
Cr	1.30	0.130	0.120	0.112	0.133	0.181(Cr ₊) -0.008(Cr ₋) 0.0865(Cr _{Avg})
Hf	1.67	—	0.700	0.990	—	0.8365
Mo	1.39	0.421	0.435	0.480	0.357	0.4053
Nb	1.46	—	0.645	0.697	3.673	0.6123
Re	1.37	—	—	—	—	0.3903
Ru	1.34	—	—	—	—	0.3912
Ta	1.49	—	0.630	0.697	0.593	0.5859
Ti	1.45	0.360	0.340	0.424	-1.222	0.3390
W	1.41	0.421	0.412	0.448	0.215	0.4088

III. LATTICE DISTORTIONS

Introduction of solute atoms leads to redistribution of electron density and lattice distortions. The total lattice distortions can be separated into two contributions. One is the macroscopic lattice distortion represented by the overall lattice parameter change of an alloy. The other is local lattice distortion. The average lattice parameter change, Δ*a*, can be determined by

$$\Delta a = a_{\text{sol}} - a_{\text{pure}} \quad [1]$$

where *a*_{pure} is the lattice parameter of pure solvent and *a*_{sol} is that of the solution containing solution atoms. Although Δ*a* is generally a nonlinear function of composition,^[11] a linear approximation is reasonable for dilute solutions; *i.e.*,

$$\Delta a = \sum_i x_i k_i \quad [2]$$

$$a_{\text{sol}} = a_{\text{pure}} + \sum_i x_i k_i \quad [3]$$

where *x_i* is the mole fraction of solute atom *i*, and *k_i* is the linear regression coefficient. In this work, we determine *k_i* by first-principles calculations using supercells by the following equation:

$$k_i = N(a_i - a_0) \quad [4]$$

where *a_i* is the calculated lattice parameter of the cell containing one solute atom *i*, *N* is the number of atoms in the supercell, and *a*₀ denotes the calculated lattice parameter for the pure solvent. The results from first-principles calculations are shown in Table I, and the linear regression coefficients for the ten solute atoms are listed in Table II.

Empirically, for a known crystal structure, the lattice parameter is related to the atomic radius, so the dependence of an alloy lattice parameter on the solute composition is typically explained by the atomic radius of solute atoms. For example, the lattice parameter of a solvent is expected to increase when solute atoms of larger atomic radius are added. In Table II, the atomic radii of the solute atoms are compared with their effects on the lattice parameter of fcc Ni. All ten solute elements have larger atomic size than Ni, and they all increase the Ni lattice parameter, as expected. In general, the amount of lattice parameter increases with the size of the atomic radius of the solute atom. However, this empirical relation is not always observed. For example, the atomic radius of Al (1.43 Å) is larger than that of Re (1.37 Å)^[9] while the lattice parameter increase due to the addition of Al atoms ($k_{Al} = 0.1587$) is considerably smaller than that caused by Re ($k_{Re} = 0.3903$). This may not be surprising because it is commonly known that the radius of an atom depends on the environment. The atomic radius is typically defined as one half of the internuclear distance between two adjacent atoms at equilibrium. Such a definition is not scientifically rigorous and the values are at best approximate. A more accurate prediction of atomic radius must take into account the interactions between the solute and solvent atoms during alloying, *i.e.*, local charge transfer and local distortion. One thus must differentiate the classic atomic radii measured in pure elements and those in alloys.

All solutes considered except Al are transition elements, and their outermost electron structures consist of *s* and *d* electrons. In Figure 1, the differences of atomic radii between solute atoms and solvent atom (Ni) are plotted with the linear regression coefficients of lattice parameters according to their periods (Figure 1(a)) and groups (Figure 1(b)) in the periodic table. It is shown that for solutes within the same period, the lattice parameter increases with the increase in the solute atom radius, although the relation is not linear. Figure 2 shows the electronic charge density of Nb, Mo, and Ru on the (001) planes of the Ni host lattice. All three elements belong to period 5. The following observations can be made: (1) the charge density of Nb shows a clear interaction along the $\langle 110 \rangle$ directions with the nearest neighbor Ni atoms; (2) the Mo *d* electrons are highly localized and less chemically active due to their half-filled *d* shell; and (3) the more outermost electrons of Ru has a higher and wider distribution of charge density, which represents a stronger interaction between Ru and neighboring Ni. Comparing with Nb and Ru, Mo has a much weaker interaction with neighboring atoms, indicating an easier compression. As a result, the data point for Mo deviates from the line connecting the Nb and Ru data points in Figure 2. In a given group, the outermost electron structures are usually similar for all elements, so the interactions between those elements (solute) and Ni (solvent) are expected to be similar. In this case, the lattice parameter change is expected to have a close correlation with the atomic radius of the solute element. Indeed, it is found that the effect of solute atoms in group 4 (Ti and Hf) and group 6 (Cr, Mo, and W) on

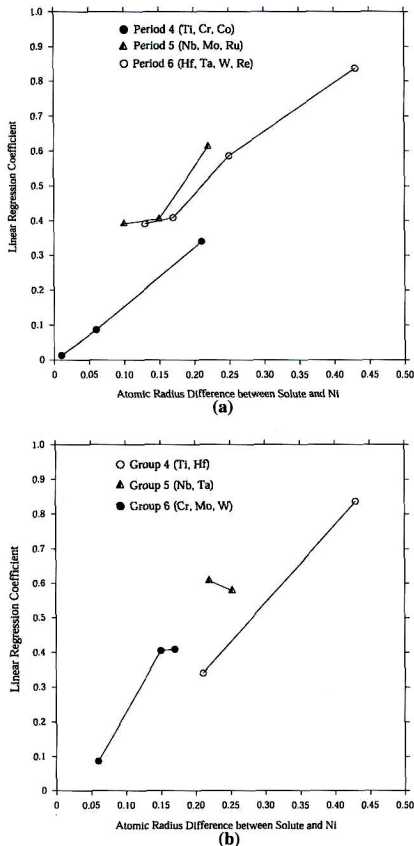


Fig. 1—Atomic radius difference between solute and solve (Ni) atoms vs linear regression coefficient.

lattice parameters can be explained by their corresponding radii. However, for group 5 (Nb and Ta), such a correlation is not observed. According to Table II, the atomic radius of Nb (1.46 Å) is slightly smaller than that of Ta (1.49 Å)^[9] but the lattice expansion caused by Nb solute ($k_{Nb} = 0.6123$) is a little bit larger than that caused by Ta ($k_{Ta} = 0.5859$). This anomaly can be explained by the difference in the valance electronic structures between Nb ($4d^4 5s^1$) and Ta ($5d^3 6s^2$).^[9] The electronic charge densities of Nb and Ta solutes are shown in Figure 3. The charge density of Nb exhibits a much stronger interaction with neighboring Ni atoms than that between Ta and neighboring Ni atoms. Therefore, Nb atoms are much harder to be compressed,

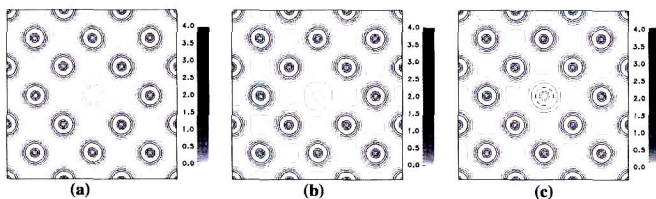


Fig. 2—Electronic charge density (in units of $e/\text{Å}^3$) of (a) Nb, (b) Mo, and (c) Ru solutes in the (001) plane of the fcc Ni lattice in period 5.

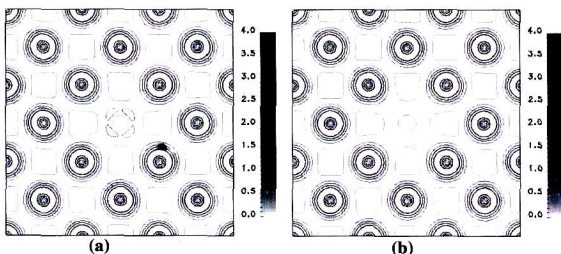


Fig. 3—Electronic charge density (in units of $e/\text{Å}^3$) of (a) Nb and (b) Ta solutes in the (001) plane of the fcc Ni lattice in group 5.

leading to a larger lattice extension than Ta in the Ni host lattice.

In addition to the electron density redistributions, the interactions between magnetic spins also contribute to lattice distortions. Repulsion is expected between spins with the same direction, and attraction will occur with opposite directions. For example, for the case of Cr substitution in fcc Ni, the atomic size difference between Cr and Ni is very small. However, there is a significant effect of Cr addition on the fcc Ni lattice parameters as a result of magnetism. When the spin direction of a Cr atom is the same as a neighboring Ni atom (Cr_{+1}), the linear regression coefficient is positive; *i.e.*, the lattice parameter increases as a result of repulsive interactions between the magnetic spins. Therefore, it is expected that if a Cr atom of opposite spin direction (Cr_{-1}) is introduced, the attractive force between magnetic spins decreases the lattice parameter, and the linear regression coefficient becomes negative.

Near a solute atom, the local distortion is generally different from the macroscopic lattice parameter change of a solid solution in magnitude and even in sign in some cases.^[10] Experimentally, the local distortions are described by the shifts in the nearest-neighbor distances around a solute atom. They can also be readily obtained using first-principles calculations by relaxing both the supercell dimensions and internal atomic positions.

Using the X-ray absorption fine structure (XAFS) technique, Scheuer and Lehgeler^[10] systematically studied the lattice distortions around impurity atoms in dilute metal alloys (the solute concentrations are between 1 and 2 at. pct). In particular, they reported

the shifts in nearest-neighbor distances of Cr, Co, Mo, Nb, and Ti in fcc Ni. We compare the experimentally measured values with those from our calculations in Table III. It is found that the calculated data agree with the experimental results within the experimental uncertainties. Among them, Co is a good example exhibiting the difference between the macroscopic lattice parameter change and the local lattice distortion. Macroscopically, Co atoms expand the fcc Ni (Table II) while locally they decrease the nearest-neighbor distances (Table III). A comparison of the calculated results for Cr_{+1} and Cr_{-1} indeed show that the spin direction has a strong effect on the local lattice distortions; *i.e.*, Cr_{-1} atoms decrease the nearest-neighbor distance and Cr_{+1} increases it.

Table III. Local Lattice Distortion in fcc Ni (in pm)

Element	Reference 10	Present Work
Al	—	1.5
Co	-0.4 ± 0.6	-0.61
Cr	-1.1 ± 0.7	1.06 (Cr_{+1}) -1.4 (Cr_{-1})
Hf	—	7.37
Mo	2.4 ± 0.3	1.92
Nb	5.4 ± 0.7	4.5
	$4.0 + 0.9$	
Re	—	1.53
Ru	—	2.74
Ta	—	4.14
Ti	2.2 ± 0.4	2.48
W	—	1.97

IV. COMPOSITION DEPENDENCE OF LATTICE PARAMETERS

Using the data shown in Tables I and II, the lattice parameters and the lattice parameter changes in the fcc-Ni solution can be predicted using Eqs. [2] and [3], respectively. The predicted results can be compared with the experimentally measured compositional dependence of lattice parameters in Ni-X binary alloys. The lattice parameter measurements were often carried out by diffraction methods. The results are usually sensitive to the experimental details and lead to significant discrepancies among data from different measurements. For example, both Taylor and Floyd^[11] and Pearson and Thompson^[12] measured the lattice parameters of Ni-Cr alloys. The results by Pearson and Thompson are 0.013 Å smaller than those by Taylor and Floyd. Such a discrepancy is significant because it is equivalent to the lattice parameter change by adding as much as 10 at. pct Cr. To reduce the systematic error within a particular measurement, we compare the measured lattice parameter changes with our calculations. In extracting the lattice parameter changes, the lattice parameter of pure Ni from the same investigation is taken as the reference. In the cases in which the data for pure Ni were not available, the linearly extrapolated value for pure Ni is used. The experimental data for binary Ni solid solutions containing Al,^[13-16] Co,^[12,17-19] Cr,^[11,12,20-23] Hf,^[23] Mo,^[23,28] Nb,^[23,29-33] Re,^[28,34] Ru,^[35-37] Ta,^[23,38] Ti,^[11,23,39-42] and W^[23,43] are used for comparison.

The calculated lattice parameter changes in Ni-Al, Ni-Co, Ni-Hf, Ni-Mo, Ni-Nb, Ni-Re, Ni-Ru, Ni-Ta, Ni-Ti, and Ni-W, together with the related experimental data, are shown in a series of plots in Figures 4 through 10. The differences are demonstrated by the standard deviations S_N , calculated as the square root of the sample variance of a set of values.^[44] Most of the

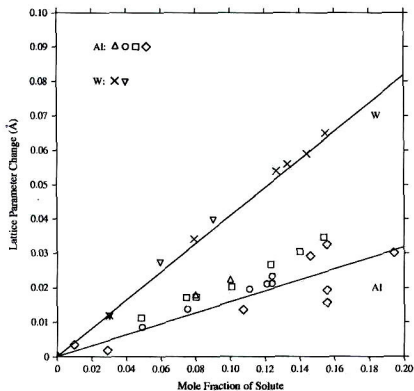


Fig. 4—Lattice parameter changes in Ni (γ) solid solutions with additions of Al and W ($S_N = 0.0059$ Å for Al and $S_N = 0.0015$ Å for W). Experimental data: Δ ,^[13] \square ,^[14] \square ,^[15] \diamond ,^[16] ∇ ,^[23] and \times ,^[43]

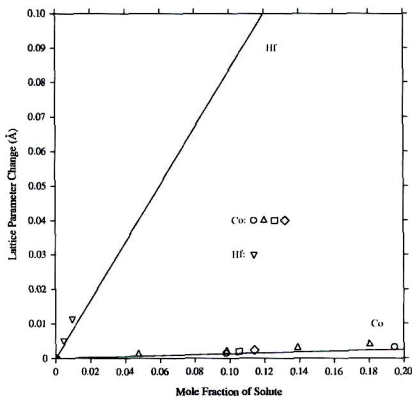


Fig. 5—Lattice parameter changes in Ni (γ) solid solutions with additions of Co and Hf ($S_N = 0.0011$ Å for Co and $S_N = 0.0017$ Å for Hf). Experimental data: Δ ,^[12] ∇ ,^[23] \square ,^[17] \square ,^[18] and \diamond ,^[19]

experimental data are well reproduced by the calculated results shown in solid lines. It is well known that both LDA and GGA lead to errors in the calculated lattice parameters as compared to experimentally measured values. However, it is also well known that the errors are systematic. Therefore, because our main interest is in the lattice parameter differences rather than the absolute values of lattice parameters, the accuracy should be much better, which is confirmed by comparisons in Figures 4 through 10. The standard deviations for Ni-Al and Ni-Ru alloys are slightly higher than others. For

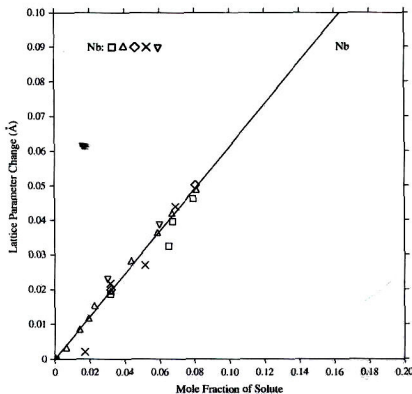


Fig. 6—Lattice parameter changes in Ni (γ) solid solutions with additions of Nb ($S_N = 0.0027$ Å for Nb). Experimental data: Δ ,^[23] \square ,^[29] ∇ ,^[30] \square ,^[32] and \times ,^[33]

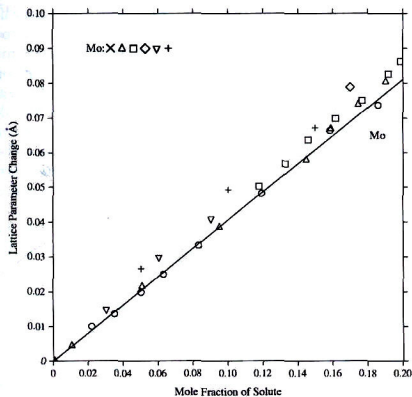


Fig. 7—Lattice parameter changes in Ni (γ) solid solutions with additions of Mo ($S_N = 0.0041 \text{ \AA}$ for Mo). Experimental data: ∇ ,^[23] \times ,^[24] Δ ,^[25] \square ,^[26] \diamond ,^[27] and $+$.^[28]

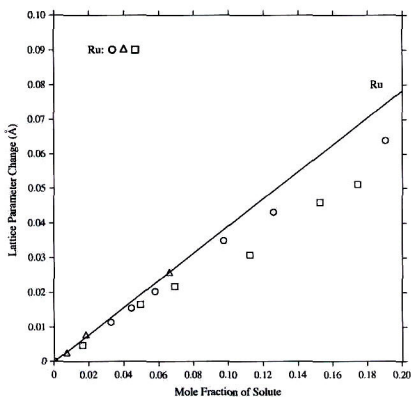


Fig. 9—Lattice parameter changes in Ni (γ) solid solutions with additions of Ru ($S_N = 0.0055 \text{ \AA}$ for Ru). Experimental data: \circ ,^[35] Δ ,^[36] and \square .^[37]

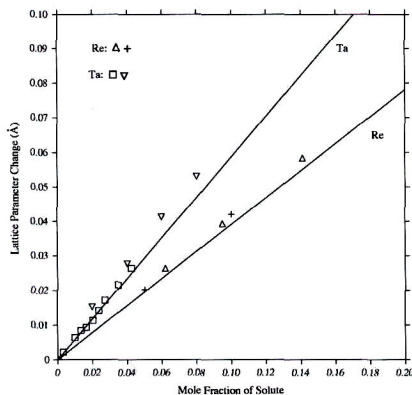


Fig. 8—Lattice parameter changes in Ni (γ) solid solutions with additions of Re and Ta ($S_N = 0.0013 \text{ \AA}$ for Re and $S_N = 0.0026 \text{ \AA}$ for Ta). Experimental data: ∇ ,^[23] $+$,^[28] Δ ,^[34] and \square .^[38]

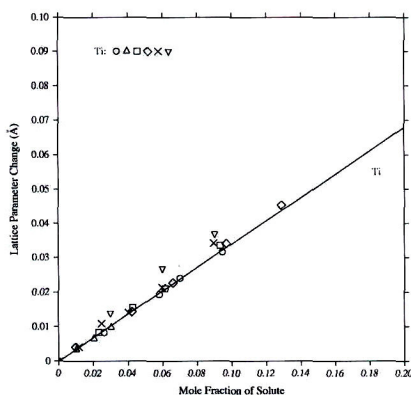


Fig. 10—Lattice parameter changes in Ni (γ) solid solutions with additions of Ti ($S_N = 0.0011 \text{ \AA}$ for Ti). Experimental data: \circ ,^[11] ∇ ,^[23] Δ ,^[39] \square ,^[40] \diamond ,^[41] and \times .^[42]

Ni-Al, the main reason is that the available experimental data are much more scattered than other systems (Figure 4). In the case of Ni-Ru, in Figure 9, the agreement between experimental data and our predictions is reasonable at low Ru concentrations (< 10 at. pct), while the large deviations are observed at high concentrations where the linear approximation (Eq. [2]) may no longer be valid. The results of calculations for " Cr_{+1} " and " Cr_{-1} " are shown in Table II and Figure 11. The linear regression coefficient for Cr_{+1} is positive, while that for Cr_{-1} is negative, because the magnetism has a significant effect on lattice distortion,

as discussed in Section III. If the system is large enough and the interaction between the two kinds of Cr atoms can be ignored, the real case can then be taken as a weighted average of the preceding two cases, which is supported by the comparison of evaluated and experimental lattice parameter changes shown in Figure 11, where all experimental data lie between the Cr_{+1} and Cr_{-1} lines. The C_{Avg} line indicates the half-half average of the Cr_{+1} and Cr_{-1} lines and is close to but a little lower than the experimental data, which means the Cr_{+1} case might have a higher possibility to occur in the real system. Our energy calculations also show that the total

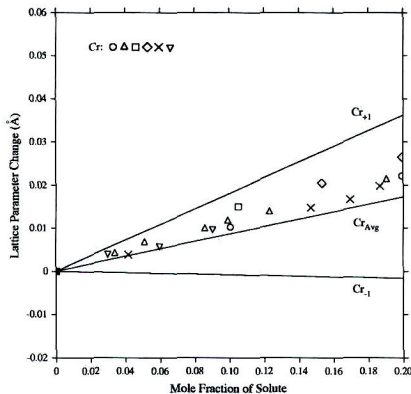


Fig. 11—Lattice parameter changes in Ni (γ) solid solutions with additions of Cr ($S_N = 0.0088 \text{ \AA}$ for Cr_{AVG}). Experimental data: \circ , \triangle , \square , \diamond , ∇ , \times , and ∇ .

energy of the Cr_{+1} system is a little bit lower (200 J/mol) than the Cr_{-1} system (Table I).

There are a number of previous investigations^[23,45-47] in the literature evaluating the linear regression coefficients of some solute atoms in fcc-Ni by fitting to the experimental data. Mishima *et al.*^[23] evaluated the linear regression coefficients from experimentally determined lattice parameters in Ni-X binary systems, and the other three investigations^[45,46,47] are based on the data from multicomponent nickel alloys. Harada and Yamazaki^[46] assumed the coefficients of the corresponding alloying elements to be the same for both the γ and the γ' phases, while Watanabe and Kuno^[45] treated them as different. Svetlov *et al.*^[47] introduced some higher order parameters in their model to describe the interaction of different solute elements. Their linear regression coefficients are summarized in Table II. As shown in Table II, the linear regression coefficients determined by the present work are very close to those given by the

three earlier investigations.^[23,45,46] Svetlov's results^[47] are somewhat different from others, even being inconsistent with some experimental information. For example, their strong negative linear regression coefficient for Ti indicates a significant decrease in lattice parameter, but the experiments show that adding Ti atoms will expand the fcc Ni lattice (Figure 10).

Lattice parameters of several Ni-Al-Cr-Co-Mo-Nb-Re-Ta-Ti-W alloys are calculated by Eq. [3], and two sets of linear regression coefficients (Mishima's^[23] and ours) are used in the calculation. Because the linear regression coefficient for Re was not determined by Mishima *et al.*,^[23] a value of 0.413 is given by fitting the experimental data shown in Figure 8. The calculated results are compared with the experimental data^[48-52] in Table IV, and the standard deviations S_N are also given. The standard deviations for two different sets of coefficients are almost the same (-0.02 \AA), which confirms again the validity of our first-principles approach in the analysis of lattice parameter change caused by solute additions. The lattice parameter data reported by Li and Wahi^[49] and Volkl^[50] cannot be well reproduced by present calculations, and some possible reasons are as follows: (1) the measurement uncertainty due to the experimental details, (2) the invalidation of the linear relationship, and (3) the interaction between different solute atoms. The last two reasons are caused by solute high concentrations.

V. SUMMARY

In this paper, we present a first-principles approach to study both the macroscopic and local lattice distortions caused by the solute atoms and apply it to the fcc-Ni lattice with Cr, Co, Mo, W, Ta, Re, Ru, Nb, Al, Ti, and Hf as solutes. The effects of atomic size, electronic interaction, and magnetic spin direction on the lattice distortions were analyzed by examining electronic charge density distributions. The calculated lattice parameter changes and the local distortions in Ni-X alloys agree well with the available experimental data in the literature, which demonstrated the validity of the approach. Using the linear regression coefficients from

Table IV. Comparison of Calculated and Experimental Lattice Parameter in Ni-Base Superalloys

Composition (At. pct)											Lattice Parameter (\AA)		
Al	Cr	Co	Mo	Nb	Re	Ta	Ti	W	Ni	Ref.	Exp.	23	Present Work
9.00	17.83	10.80	1.55	0.00	2.05	0.43	0.64	1.58	56.12	48	3.579	3.5923	3.5806
9.41	17.23	10.72	1.54	0.00	2.31	0.50	0.63	1.81	55.85		3.584	3.5949	3.5830
4.62	28.58	11.09	1.79	0.58	0.00	0.54	1.24	0.77	50.79	49	3.556	3.5923	3.5788
6.55	24.90	9.27	1.79	0.82	0.00	0.98	1.99	0.46	53.24		3.553	3.5981	3.5838
7.36	24.83	9.40	1.67	0.56	0.00	0.40	1.94	0.58	53.26		3.553	3.5935	3.5799
7.79	24.25	9.28	1.79	0.82	0.00	0.90	2.25	0.51	52.41		3.554	3.6005	3.5858
7.37	23.76	9.49	1.67	0.77	0.00	0.65	2.04	0.74	53.51		3.554	3.5967	3.5827
6.80	24.85	9.08	1.74	0.67	0.00	0.58	1.96	0.87	53.45		3.558	3.5961	3.5822
5.21	25.78	21.26	0.55	0.00	1.29	0.06	0.24	1.02	44.58	50	3.600	3.5812	3.5700
2.58	8.05	9.35	0.56	0.00	8.72	0.36	0.08	2.60	67.70	51	3.583	3.5931	3.5856
3.50	19.80	18.40	0.70	0.00	2.70	0.30	0.30	2.70	51.60	52	3.588	3.5866	3.5763
S_N												0.0221	0.0205

the first-principles calculations, the lattice parameters in multicomponent Ni-base superalloys are predicted and compared with available experimental observations, and good agreements are observed when the concentrations of individual solutes are not too high. The proposed computational approach can be employed to predict the lattice parameter changes of Ni-base alloys as a result of adding new elements, and thus can potentially be used to guide alloy development.

ACKNOWLEDGMENTS

The authors are grateful for the financial support from the NASA UEET program under Grant No. NCC3-920 and the National Science Foundation through Grant Nos. DMR-9983532, DMR-0122638, and DMR-0205232.

REFERENCES

1. T. Wang, J.Z. Zhu, R.A. Mackay, L.Q. Chen, and Z.K. Liu: *Metall. Mater. Trans. A*, 2004, vol. 35A, pp. 2313-21.
2. G. Kresse and J. Hafner: *Phys. Rev. B*, 1993, vol. 48, pp. 13115-13118.
3. J.P. Perdew: in *Electronic Structure of Solids*, P. Ziesche and H. Eschrig, eds. Akademie Verlag, Berlin, 1991.
4. R.O. Jones and O. Gunnarsson: *Rev. Mod. Phys.*, 1989, vol. 61, pp. 689-46.
5. A. Lindbaum, J. Hafner, E. Gratz, and S. Heathman: *J. Phys.-Condens. Matter*, 1998, vol. 10, pp. 2933-45.
6. A. Lindbaum, J. Hafner, and E. Gratz: *J. Phys.-Condens. Matter*, 1999, vol. 11, pp. 1177-87.
7. N. Sandberg, B. Magyari-Kope, and T.R. Mattsson: *Phys. Rev. Lett.*, 2002, vol. 89, p. 65901.
8. G. Kresse and J. Furthmuller: VASP the GUIDE, <http://cms.mpi.univie.ac.at/vasp/vasp.html>.
9. C. Counterman: *Periodic Table of the Elements*, <http://web.mit.edu/3.091/www/pt/pt1.html>.
10. U. Scheuer and B. Lengeler: *Phys. Rev. B*, 1991, vol. 44, pp. 9883-94.
11. A. Taylor and R.W. Floyd: *J. Inst. Met.*, 1951-52, vol. 80, pp. 577-87.
12. W.B. Pearson and L.T. Thompson: *Can. J. Phys.*, 1957, vol. 35, pp. 349-57.
13. A.J. Bradley and A. Taylor: *Proc. R. Soc. A*159 (1937), pp. 56-72.
14. A. Taylor and R.W. Floyd: *J. Inst. Met.*, 1952-53, vol. 81, pp. 25-32.
15. H.A. Moreen, R. Taggart, and D.H. Polonis: *Metall. Trans.*, 1971, vol. 2, pp. 265-68.
16. J. Bottiger, N. Karpe, J.P. Krog, and A.V. Ruban: *J. Mater. Res.*, 1998, vol. 13, pp. 1717-23.
17. A. Taylor: *J. Inst. Met.*, 1950, vol. 77, pp. 585-94.
18. M. Hnilicka and I. Karmazin: *Scripta Metall.*, 1974, vol. 8, pp. 1029-32.
19. J. Bandyopadhyay and K.P. Gupta: *Cryogenics*, 1977, vol. 17, pp. 345-47.
20. B.M. Rovinsky, A.I. Samoilov, and G.M. Rovinsky: *Fiz. Met. Metalloved.*, 1959, vol. 7, pp. 79-90.

21. I.I. Kornilov and A.Y. Snetkov: *Issled. Zharoproch. Splyvam, Akad. Nauk SSSR, Inst., Met. Im. A.A. Baikova*, 1961, vol. 7, pp. 106-11.
22. L. Karmazin and M. Svoboda: *Kovove Mater.*, 1979, vol. 17, pp. 355-62.
23. Y. Mishima, S. Ochiai, and T. Suzuki: *Acta Metall.*, 1985, vol. 33, pp. 1161-69.
24. W. Koster and W. Schmidt: *Arch. Eisenhüttenwes.*, 1934, vol. 8, pp. 25-27.
25. G. Grube and H. Schlecht: *Z. Elektrochem.*, 1938, vol. 44, pp. 413-22.
26. P.W. Guthrie and E.E. Stansbury: Report No. ORNL-3078, Oak Ridge National Laboratory, Oak Ridge, TN, 1961.
27. R.E.W. Casselton and W. Hume-Rothery: *J. Less-Common Met.*, 1964, vol. 7, pp. 212-21.
28. A.S. Pavlovic, V.S. Babu, and M.S. Seehra: *J. Phys.-Condens. Matter*, 1996, vol. 8, pp. 3139-49.
29. G. Grube, O. Kubaschewski, and K. Zwiauer: *Z. Elektrochem.*, 1939, vol. 45, pp. 881-84.
30. S. Arajs, H. Chessin, and R.V. Colvin: *Phys. Status Solidi*, 1963, vol. 3, pp. 2337-46.
31. I.J. Duerden and W. Hume-Rothery: *J. Less-Common Met.*, 1966, vol. 11, pp. 381-87.
32. L.N. Guseva, R.S. Mints, and E.S. Malkov: *Russ. Metall.*, 1969, vol. 5, pp. 120-22.
33. D.S. Duvall and J.M.J. Donachie: *J. Inst. Met.*, 1970, vol. 98, pp. 182-87.
34. E.M. Savitskii, M.A. Tylkina, and E.P. Arskaya: *Izv. V.U.Z. Tsv. Metall.*, 1970, vol. 4, pp. 114-16.
35. E. Raub and D. Menzel: *Z. Metallkd.*, 1961, vol. 52, pp. 831-33.
36. W.L. Phillips: *Trans. TMS-AIME*, 1964, vol. 230, pp. 526-29.
37. I.I. Kornilov and K.P. Myasnikova: *Izv. Akad. Nauk SSSR, Met. Govn. Delo*, 1964, pp. 159-65.
38. H. Chessin, S. Arajs, and R.V. Colvin: *J. Appl. Phys.*, 1964, vol. 35, pp. 2419-23.
39. T.H. Hazlett and E.R. Parker: *Trans. ASM*, 1954, vol. 46, pp. 701-15.
40. D. M. Poole and W. Hume-Rothery: *J. Inst. Met.*, 1954-55, vol. 83, pp. 473-80.
41. K. Hashimoto, T. Tsujimoto, and K. Saito: *Trans. Jpn. Inst. Met.*, 1981, vol. 22, pp. 798-806.
42. G. Chattopadhyay and H. Kleykamp: *Z. Metallkd.*, 1983, vol. 74, pp. 182-97.
43. E. Epreman and D. Harker: *Trans. AIME*, 1949, vol. 185, pp. 267-73.
44. J.F. Kenney and E.S. Keeping: *Mathematics of Statistics, Pt. 1*, 3rd ed., Princeton, New York, 1962.
45. R. Watanabe and T. Kuno: *Tetsu-to-Hagané*, 1975, vol. 61, pp. 2274-94.
46. H. Harada and M. Yamazaki: *Tetsu-to-Hagané*, 1979, vol. 65, pp. 1059-68.
47. I.L. Svetlov, I.V. Oldakovskii, N.V. Petrushin, and I.A. Ignatova: *Russ. Metall.*, 1991, pp. 139-45.
48. D.F. Lahrman, R.D. Field, R. Darolia, and H.L. Fraser: *Acta Metall.*, 1988, vol. 36, pp. 1309-20.
49. J. Li and R.P. Wahi: *Acta Metall. Mater.*, 1995, vol. 43, pp. 507-17.
50. R. Volk, U. Glatzel, and N. Feller-Kniepmeier: *Scripta Mater.*, 1998, vol. 38, pp. 893-900.
51. C. Schulze and M. Feller-Kniepmeier: *Mater. Sci. Eng. A*, 2000, vol. 281, pp. 204-12.
52. D. Sieborger, H. Brehm, F. Wunderlich, D. Moller, and U. Glatzel: *Z. Metallkd.*, 2001, vol. 92, pp. 58-61.